Article

# Understanding and Predicting Distorted T- versus Y-Geometries for Neutral Chromous Complexes Supported by a Sterically Encumbering #-Diketiminate Ligand

Hongjun Fan, Debashis Adhikari, Anas A. Saleh, Rodney L. Clark, Francisco J. Zuno-Cruz, Gloria Sanchez Cabrera, John C. Huffman, Maren Pink, Daniel J. Mindiola, and Mu-Hyun Baik

*J. Am. Chem. Soc.*, **2008**, 130 (51), 17351-17361 • DOI: 10.1021/ja803798b • Publication Date (Web): 26 November 2008



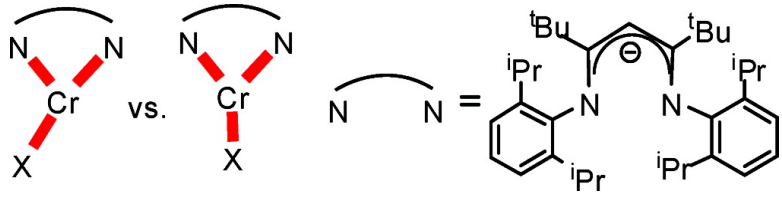


## More About This Article

Additional resources and features associated with this article are available within the HTML version:

- Supporting Information
- Access to high resolution figures
- Links to articles and content related to this article
- Copyright permission to reproduce figures and/or text from this article

View the Full Text HTML

J|A|C|S
ARTICLES

Published on Web 11/26/2008

# Understanding and Predicting Distorted T- versus Y-Geometries for Neutral Chromous Complexes Supported by a Sterically Encumbering $\beta$-Diketiminate Ligand

Hongjun Fan,[†] Debashis Adhikari,[†] Anas A. Saleh,[†] Rodney L. Clark,[†] Francisco J. Zuno-Cruz,[‡] Gloria Sanchez Cabrera,[‡] John C. Huffman,[†] Maren Pink,[†] Daniel J. Mindiola,*[,†] and Mu-Hyun Baik*[,†]

*Department of Chemistry, the Molecular Structure Center, and School of Informatics, Indiana University, Bloomington, Indiana 47405, and Centro de Investigaciones Químicas, Universidad Autónoma del Estado de Hidalgo, Ciudad Universitaria, Km 4.5 Carretera Pachuca-Tulancingo, Pachuca, Estado de Hidalgo, 42184, Mexico*

Received May 21, 2008; E-mail: mindiola@indiana.edu; mbaik@indiana.edu

***Abstract:*** A series of three-coordinate Cr(II) complexes sharing the common molecular fragment "(nacnac)Cr" (nacnac$^-$ = [ArNC($^t$Bu)]$_2$CH, Ar = 2,6-$^i$Pr$_2$C$_6$H$_3$) were prepared via salt metathesis with the dimer [(nacnac)Cr($\mu$-Cl)]$_2$. Single-crystal X-ray diffraction studies revealed that the complexes (nacnac)Cr(L) (L = CH$_2$$^t$Bu, CH$_3$, CH$_2$CH$_3$, SiH{2,4,6-Me$_3$C$_6$H$_2$}$_2$, O{2,6-$^i$Pr$_2$C$_6$H$_3$}, N{CH$_3$}$_2$) represent a rare class of mononuclear, neutral chromium complexes with a three-coordinate high-spin chromous metal center. Depending on the nature of the third ligand, L$^-$, these complexes can adopt either distorted T-shaped or Y-shaped coordination geometries. Density functional theory calculations and molecular orbital analyses in combination with a detailed molecular fragment energy decomposition were used to establish an intuitive concept of the key electronic structure patterns that determine the coordination geometry of preference. The frontier orbitals of the (nacnac)Cr(II) fragment direct $\pi$-donating ligands to adopt Y-shaped geometry, whereas ligands that are primarily $\sigma$-donors prefer T-shaped coordination. The relationship between electronics at the metal center and coordination geometry was extended to include the putative neutral three-coordinate high-spin complexes of Sc(II) and Mn(II), which are predicted to both adopt Y-shaped geometry.

## Introduction

Recently, $\beta$-diketiminate complexes of Cr(III) have received much attention because they may serve as structural and functional models[1−3] of the alleged active sites of the heterogeneous Phillips ethylene polymerization catalyst (Cr/SiO$_2$).[4] Despite significant efforts in the past, little is known about the chemical nature of the catalytically competent Cr center to date, making a rational approach to designing more efficient chromium catalysts difficult. One common feature shared by a number of systems that are being studied is that the active complexes consist of a Cr(III) center in low-coordination environment. Recently, Theopold and co-workers established that unsaturated Cr(III) cations could be generated upon one-electron oxidation of Cr(II), and the formal systems were found to be efficient single-site catalysts for the polymerization of ethylene.[5a] Inspired by the work of Theopold[1,5] and Gibson,[2] we sought to investigate the relationship between electronic structure and coordination geometry of chromium(II) complexes using a sterically demanding $\beta$-diketiminate ligand nacnac$^-$ (nacnac$^-$ = [ArNC($^t$Bu)]$_2$CH, Ar = 2,6-$^i$Pr$_2$C$_6$H$_3$). Starting from [(nacnac)Cr($\mu$-Cl)]$_2$, we were able to prepare and characterize a number of rare three-coordinate (distorted T-shaped or Y-shaped), neutral Cr(II) complexes (nacnac)Cr(R) (R = CH$_2$$^t$Bu, CH$_3$, Et, SiH{2,4,6-Me$_3$C$_6$H$_2$}$_2$, O{2,6-$^i$Pr$_2$C$_6$H$_3$}, and N{CH$_3$}$_2$) that are formed by salt metathesis.

Understanding how different coordination geometries can be accessed by modifying the ligand composition is interesting on fundamental grounds and is crucial for rational catalyst design. For example, a T-shaped coordination environment is in

[†] Indiana University.
[‡] Universidad Autónoma del Estado de Hidalgo.

(1) (a) Theopold, K. H. *Acc. Chem. Res.* **1990**, *23*, 263–270. (b) Pariya, C.; Theopold, K. H. *Curr. Sci.* **2000**, *78*, 1345–1351. (c) Kim, W.-K.; Fevola, M. J.; Liable-Sands, L. M.; Rheingold, A. L.; Theopold, K. H. *Organometallics* **1998**, *17*, 4541–4543. (d) MacAdams, L. A.; Kim, W.-K.; Liable-Sands, L. M.; Guzei, I. A.; Rheingold, A. L.; Theopold, K. H. *Organometallics* **2002**, *21*, 952–960.

(2) (a) Gibson, V. C.; Newton, C.; Redshaw, C.; Solan, G. A.; White, A. J. P.; Williams, D. J.; Maddox, P. J. *Chem. Commun.* **1998**, 1651–1652. (b) Gibson, V. C.; Newton, C.; Redshaw, C.; Solan, G. A.; White, A. J. P.; Williams, D. J. *Eur. J. Inorg. Chem.* **2001**, 1895–1903.

(3) For other examples of $\beta$-diketiminate Cr(III) complexes, see: (a) Cotton, F. A.; Czuchajowska, J.; Feng, X. *Inorg. Chem.* **1990**, *29*, 4329–4335. (b) Cotton, F. A.; Czuchajowska, J.; Falvello, L. R.; Feng, X. *Inorg. Chim. Acta* **1990**, *172*, 135–136.

(4) (a) Hogan, J. P. *J. Polym. Sci., Polym. Ed.* **1970**, *8*, 2637–2652. (b) Karol, F. J.; Karapinka, G. L.; Wu, C.; Dow, A. W.; Johnson, R. N.; Carrick, W. L. *J. Polym. Sci., Part A* **1972**, *10*, 2621–2637. (c) McDaniel, M. P. *Adv. Catal.* **1985**, *33*, 47–98. (d) Ajjou, J. A. N.; Scott, S. L.; Paquet, V. *J. Am. Chem. Soc.* **1998**, *120*, 415–416.

(5) (a) MacAdams, L. A.; Buffone, G. P.; Incarvito, C. D.; Rheingold, A. L.; Theopold, K. H. *J. Am. Chem. Soc.* **2005**, *127*, 1082–1083. (b) MacAdams, L. A.; Buffone, G. P.; Incarvito, C. D.; Golen, J. A.; Rheingold, A. L.; Theopold, K. H. *Chem. Commun.* **2003**, 1164–1165.

  

principle the most desirable geometry for the resting state of the catalyst, as substrate uptake to afford a square-planar four-coordinate reactant complex will be straightforward owing to the empty coordination site at the reactive metal center. The Y-shaped structure is expected to be less reactive toward reactant complex formation in certain cases but may offer the advantage of preventing unproductive side reactions in the later part of the catalysis. Trigonal planar systems[6] do, however, display unparalleled reactivity in the context of three-coordinate group 4 imides given their ability to promote intermolecular C−H activation of arenes and alkanes, which also includes methane.[7] Likewise, three-coordinate group 5 systems supported by sterically demanding silox ligands (silox = $^{-}$OSi$^{t}$Bu$_3$) have been demonstrated to promote reductive cleavage of strong bonds such as CO and the N−C linkage in anilines and pyridine.[8] Three-coordinate tungsten systems complement the group 4 metals with their prominent role in intermolecular C−H activation of arenes.[9] This type of chemistry is not only restricted to C−H bonds alone because $C_3$ symmetric three-coordinate molybdenum complexes supported by sterically encumbering anilides can incite the activation and reductive cleavage of atmospheric nitrogen under normal conditions (1 atm, 25 °C).[10] When invoking the later metals, three-coordinate templates play pivotal roles in catalytic and stoichiometric group transfer reactions,[11−13] in addition to providing useful models for the reactive sites in metalloenzymes such as nitrogenase[14] and type 1 copper biological electron-transfer manifolds.[15] In unrelated work, we demonstrated previously how controlling the coordination geometry of the metal site is critical for harnessing the reactive power of transition metal complexes toward small molecule activation.[16] Intuitively, it is not clear which electronic features could be exploited to control the formation of the Y- versus T-shaped coordination geometry in three-coordinate Cr(II) complexes. The goal of this study is to establish such conceptual strategy combining theory and experiment, as well as theoretically predict the geometrical preference for three-coordinate fragments that remain unknown.[17]

## Experimental Details

**General Considerations.** Unless otherwise stated, all experiments were performed in a M. Braun Laboratory Master double-dry box under an atmosphere of purified nitrogen or using high vacuum standard Schlenk techniques under an argon atmosphere.[18] Anhydrous *n*-hexane, pentane, toluene, and benzene were purchased from Aldrich in sure-sealed reservoirs (18 L) and further dried by passage through two columns of activated alumina and a Q-5 column.[19] Diethylether and $CH_2Cl_2$ were dried by passage through two columns of activated alumina.[19] THF was distilled, under nitrogen, from purple sodium benzophenone ketyl and stored over sodium metal. Distilled THF was collected in a thick walled collection flask under inert atmosphere and transferred to a glove box. $C_6D_6$ was purchased from Cambridge Isotope Laboratory (CIL), degassed, and dried over $CaH_2$, and then vacuum transferred to 4 Å molecular sieves. Celite, alumina, and 4 Å molecular sieves were activated under vacuum overnight at 200 °C. Li(nacnac),[20] LiCH$_2$$^{t}$Bu,[21] and (THF)$_2$LiSiH{2,4,6-Me$_3$C$_6$H$_2$}$_2$[22] were prepared according to the literature. NaO{2,6-$^{i}$Pr$_2$C$_6$H$_3$} was prepared by addition of NaN{Si(CH$_3$)$_3$}$_2$ to a −35 °C ether solution of HO{2,6-$^{i}$Pr$_2$C$_6$H$_3$}. The white solid was filtered, washed with ether, and dried under reduced pressure. All other reagents were used as received. CHN analyses were performed by Desert Analytics, Tucson, AZ, and Midwest Microlabs, Indianapolis, IN. $^1$H NMR spectra were recorded on Varian 400 or 300 MHz NMR spectrometers. $^1$H NMR spectra are reported with reference to solvent resonances (residual $C_6D_5H$ in $C_6D_6$, 7.16 ppm). Electronic absorption spectra were obtained with a Perkin-Elmer Lamba 19 spec-


(6) For an extensive review on three-coordinate metal complexes, see: Cummins, C. C. *Prog. Inorg. Chem.* **1998**, *47*, 685–836.

(7) (a) Cummins, C. C.; Baxter, S. M.; Wolczanski, P. T. *J. Am. Chem. Soc.* **1988**, *110*, 8731. (b) Cummins, C. C.; Schaller, C. P.; Van Duyne, G. D.; Wolczanski, P. T.; Chan, A. W. E.; Hoffmann, R. *J. Am. Chem. Soc.* **1991**, *113*, 2985. (c) Bennett, J. L; Wolczanski, P. T. *J. Am. Chem. Soc.* **1994**, *116*, 2179–2180. (d) Schaller, C. P.; Bonanno, J. B.; Wolczanski, P. T. *J. Am. Chem. Soc.* **1994**, *116*, 4133–4134. (e) Slaughter, L. M.; Wolczanski, P. T.; Klinckman, T. R.; Cundari, T. R. *J. Am. Chem. Soc.* **2000**, *122*, 7953–7975. (f) Schaller, C. P.; Cummins, C. C.; Wolczanski, P. T. *J. Am. Chem. Soc.* **1996**, *118*, 591–611. (g) Bennett, J. L.; Wolczanski, P. T. *J. Am. Chem. Soc.* **1997**, *119*, 10696–10719. (h) Cundari, T. R.; Klinckman, T. R.; Wolczanski, P. T. *J. Am. Chem. Soc.* **2002**, *124*, 1481–1487.

(8) (a) LaPointe, R. E.; Wolczanski, P. T.; Mitchell, J. F. *J. Am. Chem. Soc.* **1986**, *108*, 6382–6384. (b) Neithamer, D. R.; LaPointe, R. E.; Wheeler, R. A.; Richeson, D. S.; Van Duyne, G. D.; Wolczanski, P. T. *J. Am. Chem. Soc.* **1989**, *111*, 9056–9072. (c) Kleckley, T. S.; Bennett, J. L.; Wolczanski, P. T.; Lobkovsky, E. B. *J. Am. Chem. Soc.* **1997**, *119*, 247–248. (d) Bonanno, J. B.; Henry, T. P.; Neithamer, D. R.; Wolczanski, P. T.; Lobkovsky, E. B. *J. Am. Chem. Soc.* **1996**, *118*, 5132–5133.

(9) Schafer, D. F.; Wolczanski, P. T. *J. Am. Chem. Soc.* **1998**, *120*, 4881–4882.

(10) (a) Laplaza, C. E.; Cummins, C. C. *Science* **1995**, *268*, 861–863. (b) Laplaza, C. E.; Johnson, M. J. A.; Peters, J. C.; Odom, A. L.; Kim, E.; Cummins, C. C.; George, G. N.; Pickering, I. J. *J. Am. Chem. Soc.* **1996**, *118*, 8623–8638. (c) Peters, J. C.; Cherry, J.-P. F.; Thomas, J. C.; Baraldo, L.; Mindiola, D. J.; Davis, W. M.; Cummins, C. C. *J. Am. Chem. Soc.* **1999**, *121*, 10053–10067.

(11) (a) Mindiola, D. J.; Hillhouse, G. L. *J. Am. Chem. Soc.* **2001**, *123*, 4623–4624. (b) Mindiola, D. J.; Hillhouse, G. L. *J. Am. Chem. Soc.* **2002**, *124*, 9976–9977. (c) Melenkivitz, R.; Mindiola, D. J.; Hillhouse, G. L. *J. Am. Chem. Soc.* **2002**, *124*, 3846–3847. (d) Waterman, R.; Hillhouse, G. L. *J. Am. Chem. Soc.* **2003**, *125*, 13350–13351.

(12) (a) Kogut, E.; Wiencko, H. L.; Zhang, L.; Cordeau, D. E.; Warren, T. H. *J. Am. Chem. Soc.* **2005**, *127*, 11248–11249. (b) Dai, X.; Kapoor, P.; Warren, T. H. *J. Am. Chem. Soc.* **2004**, *126*, 4798–4799.

(13) Vela, J.; Smith, J. M.; Yu, Y.; Ketterer, N. A.; Flaschenriem, C. J.; Lachicotte, R. J.; Holland, P. L. *J. Am. Chem. Soc.* **2005**, *127*, 7857–7870.

(14) (a) Smith, J. M.; Lachicotte, R. J.; Pittard, K. A.; Cundari, T. R.; Lukat-Rodgers, G.; Rodgers, K. R.; Holland, P. L. *J. Am. Chem. Soc.* **2001**, *123*, 9222–9223. (b) Smith, J. M.; Lachicotte, R. J.; Holland, P. L. *J. Am. Chem. Soc.* **2003**, *125*, 15752–15753. (c) Vela, J.; Stoian, S.; Flaschenriem, C. J.; Munck, E.; Holland, P. L. *J. Am. Chem. Soc.* **2004**, *126*, 4522–4523. (d) Andres, H.; Bominaar, E. L.; Smith, J. M.; Eckert, N. A.; Holland, P. L.; Munck, E. *J. Am. Chem. Soc.* **2002**, *124*, 3012–3025. (e) Smith, J. M.; Sadique, A. R.; Cundari, T. R.; Rodgers, K. R.; Lukat-Rodgers, G.; Lachicotte, R. J.; Flaschenriem, C. J.; Vela, J.; Holland, P. L. *J. Am. Chem. Soc.* **2006**, *128*, 756–769.

(15) (a) Holland, P. L.; Tolman, W. B. *J. Am. Chem. Soc.* **1999**, *121*, 7270–7271. (b) Holland, P. L.; Tolman, W. B. *J. Am. Chem. Soc.* **2000**, *122*, 6331–6332. (c) Randall, D. W.; George, S. D.; Holland, P. L.; Hedman, B.; Hodgson, K. O.; Tolman, W. B.; Solomon, E. I. *J. Am. Chem. Soc.* **2000**, *122*, 11632–11648.

(16) (a) Bailey, B. C.; Fan, H.; Baum, E. W.; Huffman, J. C.; Baik, M.-H.; Mindiola, D. J. *J. Am. Chem. Soc.* **2005**, *127*, 16016. (b) Bailey, B. C.; Fan, H.; Huffman, J. C.; Baik, M.-H.; Mindiola, D. J. *J. Am. Chem. Soc.* **2007**, *129*, 8781–8793.

(17) Holland, P. L.; Cundari, T. R.; Perez, L. L.; Eckert, N. A.; Lachicotte, R. J. *J. Am. Chem. Soc.* **2002**, *124*, 14416–14424.

(18) For a general description of the equipment and techniques used in carrying out this chemistry, see: Burger, B. J.; Bercaw, J. E. In *Experimental Organometallic Chemistry*; Wayda, A. L., Darensbourg, M. Y., Eds.; ACS Symposium Series 357; American Chemical Society: Washington, D.C., 1987; pp 79−98.

(19) Pangborn, A. B.; Giardello, M. A.; Grubbs, R. H.; Rosen, R. K.; Timmers, F. J. *Organometallics* **1996**, *15*, 1518–1520.

(20) Budzelaar, P. H. M.; van Oort, A. B.; Orpen, A. G. *Eur. J. Inorg. Chem.* **1998**, 1485–1494.

(21) Schrock, R. R.; Fellmann, J. D. *J. Am. Chem. Soc.* **1978**, *100*, 3359–3370.

(22) (a) Tilley, T. D. *Organometallics* **1985**, *4*, 1452–1457. (b) Arnold, J.; Roddick, D. M.; Tilley, T. D.; Geib, S. J. *Inorg. Chem.* **1988**, *27*, 3510–3514. (c) Roddick, D. M.; Heyn, R. H.; Tilley, T. D. *Organometallics* **1989**, *8*, 324–330.

trophotometer using UVWinlab software. Solution magnetic moment measurements were obtained by the method of Evans.[23] X-ray diffraction data were collected on a SMART6000 (Bruker) system under a stream of $N_2$(g) at low temperatures.[24]

**Synthesis of Complex [(nacnac)Cr($\mu_2$-Cl)]$_2$ (1).** In a 1000 mL round-bottom flask was loaded anhydrous $CrCl_2$ (1.728 g, 14.1 mmol), and the solid was suspended in 180 mL of THF and cooled to −35 °C. To the cold suspension was added dropwise a cold THF solution (∼100 mL) containing Li(nacnac) (6.790 g, 13.4 mmol). Upon warming, the mixture gradually darkened, and the reaction was allowed to stir for 48 h at 25 °C. The dark-green solution was dried under reduced pressure, extracted with ∼300 mL of toluene, filtered, and the filtrate was concentrated (∼220 mL) and stored at −35 °C for 24 h to afford dark crystals and powder of [(nacnac)Cr($\mu_2$-Cl)]$_2$ (**1**) (4.200 g, 3.57 mmol, 53.4% yield, 4 crops). Crystallization is slow, and toluene solutions must be further concentrated to obtain more product.

For **1**: $^1$H NMR (23 °C, 399.8 MHz, $C_6D_6$) $\delta$ 11.5 ($\Delta\nu_{1/2}$ = 290 Hz), −8.87 ($\Delta\nu_{1/2}$ = 154 Hz); $\mu_{eff}$ = 2.95 $\mu_B$ per chromium center ($C_6D_6$, 298 K, Evans' method); UV−vis ($C_6H_6$, 23 °C) 367 (sh), 405 ($\epsilon$ = 10767), and 386 nm ($\epsilon$ = 6963); IR ($C_6H_6$, $CaF_2$) 2963 (m), 2869 (m), 1521 (m), 1379 (m), 1365 (s), 1318 (w), 1069 (w) cm$^{-1}$. Anal. Calcd for $C_{70}H_{106}N_4Cl_2Cr_2$: C, 71.34; H, 9.07; N, 4.76. Found: C, 71.74; H, 8.74; N, 4.78.

**Synthesis of Complex (nacnac)Cr($CH_2^tBu$) (2).** In a vial was loaded **1** (1.00 g, 0.85 mmol), and the solid was suspended in 70 mL of $Et_2O$ and cooled to −35 °C. To the cold suspension was added dropwise a cold $Et_2O$ solution (∼10 mL) containing $LiCH_2^tBu$ (146 mg, 1.87 mmol). Upon mixing, the solution changed rapidly to yellow-brown, and the reaction was allowed to stir for an additional 10 h at 25 °C. The brown solution was dried under reduced pressure, and the solids were extracted with pentane, filtered, and the filtrate was concentrated and stored at −35 °C for 24 h to afford large blocks of (nacnac)Cr($CH_2^tBu$) (**2**) (540 mg, 0.865 mmol, 51% yield, 2 crops).

For **2**: $^1$H NMR (23 °C, 399.8 MHz, $C_6D_6$) $\delta$ 10.19 ($\Delta\nu_{1/2}$ = 287 Hz), 1.10, −9.96; $\mu_{eff}$ = 5.09 $\mu_B$ ($C_6D_6$, 298 K, Evans' method); UV−vis ($C_6H_6$, 23 °C) 386 ($\epsilon$ = 2753), and 404 nm ($\epsilon$ = 3104); IR ($C_6H_6$, $CaF_2$): 2961 (m), 2869 (w), 1517 (m), 1473 (w), 1382 (s), 1364 (s), 1319 (m) cm$^{-1}$. Anal. Calcd for $C_{40}H_{64}N_2Cr$: C, 76.87; H, 10.32; N, 4.48. Found: C, 76.90; H, 10.15; N, 4.45.

**Synthesis of Complex (nacnac)Cr($CH_3$) (3).** In a vial was loaded **1** (165 mg, 0.14 mmol), and the solid was suspended in 12 mL of $Et_2O$ and cooled to −35 °C. To the cold suspension was added dropwise a cold $Et_2O$ solution (∼5 mL) containing $ClMgCH_3$ (3 M solution in THF, 107 $\mu$L, 0.32 mmol). Upon mixing, the solution changed rapidly to yellow-brown, and the reaction was allowed to stir for 0.5 h at 25 °C. The brown solution was dried under reduced pressure, and the solid was extracted with pentane, filtered, and the filtrate was concentrated and stored at −35 °C for 24 h to afford thin plates of (nacnac)Cr($CH_3$) (**3**) (83 mg, 0.15 mmol, 53% yield, 2 crops).

For **3**: $^1$H NMR (23 °C, 399.8 MHz, $C_6D_6$) $\delta$ 11.33 ($\Delta\nu_{1/2}$ = 233 Hz), −13.07 ($\Delta\nu_{1/2}$ = 55 Hz); $\mu_{eff}$ = 5.057 $\mu_B$ ($C_6D_6$, 298 K, Evans' method); UV−vis ($C_6H_6$, 23 °C) 403 ($\epsilon$ = 3823), and 305 nm ($\epsilon$ = 3358); IR ($C_6H_6$, $CaF_2$) 2962 (m), 2870 (w), 1525 (m), 1381 (s) 1365 (s) 1319 (m) cm$^{-1}$. Anal. Calcd for $C_{36}H_{56}N_2Cr$: C, 76.01; H, 9.92; N, 4.93. Found: C, 75.84; H, 9.74; N, 4.91.

**Synthesis of Complex (nacnac)Cr($CH_2CH_3$) (4).** In a vial was loaded **1** (243 mg, 0.207 mmol), and the solid was suspended in 20 mL of $Et_2O$ and cooled to −35 °C. To the cold suspension was added dropwise a cold $Et_2O$ solution (∼10 mL) containing $ClMg(CH_2CH_3)$ (2.0 M solution in $Et_2O$, 230 $\mu$L, 0.454 mmol). Upon mixing, the solution color changed rapidly to yellow-brown, and the reaction was allowed to stir for 1 h at 25 °C. The brown solution was dried under reduced pressure, and the solids were extracted with pentane, filtered, and the filtrate was concentrated and stored at −35 °C for 24 h to afford thin plates of (nacnac)Cr($CH_2CH_3$) (**4**) (138 mg, 0.237 mmol, 57% yield, 2 crops).

For **4**: $^1$H NMR (23 °C, 399.8 MHz, $C_6D_6$) $\delta$ 11.10 ($\Delta\nu_{1/2}$ = 242 Hz); $\mu_{eff}$ = 4.891 $\mu_B$ ($C_6D_6$, 298 K, Evans' method); UV−vis ($C_6H_6$, 23 °C) 282 (sh), 405 ($\epsilon$ = 3214), and 421 nm ($\epsilon$ = 2953); IR ($C_6H_6$, $CaF_2$) 2963 (m), 2929 (m), 2869 (m), 1521 (m) 1381(s) 1363 (s), 1319 (m), 1118 (m) cm$^{-1}$. Anal. Calcd for $C_{37}H_{58}N_2Cr$: C, 76.24; H, 10.03; N, 4.81. Found: C, 75.63; H, 9.54; N, 4.74.

**Synthesis of Complex (nacnac)Cr(SiH{2,4,6-Me$_3$C$_6$H$_2$}$_2$) (5).** In a vial was loaded **1** (100 mg, 0.085 mmol), and the solid was suspended in 10 mL of THF and cooled to −35 °C. To the cold suspension was added dropwise a cold THF solution (∼5 mL) of $(THF)_2$Li(SiH{2,4,6-$Me_3C_6H_2$}$_2$) (71.2 mg, 0.17 mmol). Upon mixing, the solution changed rapidly to yellow-brown, and the reaction was allowed to stir for 4 h at 25 °C. The brown solution was dried under reduced pressure, and the solid was extracted with pentane. Filtration was performed after that, and the filtrate was concentrated and stored at −35 °C for 24 h to afford large yellow blocks of (nacnac)Cr(SiH{2,4,6-$Me_3C_6H_2$}$_2$) (**5**) (89 mg, 0.107 mmol, 63% yield).

For **5**: $^1$H NMR (23 °C, 399.8 MHz, $C_6D_6$) $\delta$ 2.98 ($\Delta\nu_{1/2}$ = 173 Hz), −0.25 ($\Delta\nu_{1/2}$ = 94 Hz); $\mu_{eff}$ = 4.71 $\mu_B$ ($C_6D_6$, 298 K, Evans' method); IR ($C_6H_6$, $CaF_2$) 3071 (m), 3029 (m), 1512 (s) cm$^{-1}$. Anal. Calcd for $C_{54}H_{76}N_2CrSi$: C, 77.51; H, 9.32; N, 3.4. Found: C, 77.58; H, 8.86; N, 3.15.

**Synthesis of Complex (nacnac)Cr(O{2,6-$^i$Pr$_2$C$_6$H$_3$}) (6).** In a vial was loaded **1** (100 mg, 0.097 mmol), and the solid was suspensed in 10 mL of THF and cooled to −35 °C. To the cold suspension was added dropwise a cold THF solution (∼5 mL) containing NaO{2,6-$^i$Pr$_2$C$_6$H$_3$} (41.0 mg, 0.20 mmol). Upon mixing, the solution color changed rapidly to orange-brown, and the reaction was allowed to stir for 1.2 h at 25 °C. The brown solution was dried under reduced pressure, and the solids were extracted with hexane, filtered, and the filtrate was concentrated and stored at −35 °C for 12 h to afford large blocks of (nacnac)Cr(O{2,6-$^i$Pr$_2$C$_6$H$_3$}) (**6**) (30 mg, 0.58 mmol, 42% yield, 2 crops).

For **6**: $^1$H NMR (23 °C, 399.8 MHz, $C_6D_6$) $\delta$ 15.27 ($\Delta\nu_{1/2}$ = 73.8 Hz), 12.02 ($\Delta\nu_{1/2}$ = 293.4 Hz), 9.52 ($\Delta\nu_{1/2}$ = 28.5 Hz), −6.55 ($\Delta\nu_{1/2}$ = 313.2 Hz), −12.95 ($\Delta\nu_{1/2}$ = 84.4 Hz); $\mu_{eff}$ = 4.773 $\mu_B$ ($C_6D_6$, 298 K, Evans' method); UV−vis ($C_6H_6$, 23 °C) 432.5 ($\epsilon$ = 8796.6), 413 ($\epsilon$ = 7525.4), and 310 nm ($\epsilon$ = 12525); IR ($C_6H_6$, $CaF_2$) 3695 (m), 3641 (m), 3092 (s), 2324 (s) cm$^{-1}$. Anal. Calcd for $C_{36}H_{53}N_2CrO_3F_3S$: C, 77.22; H, 9.65; N, 3.83. Found: C, 76.97; H, 9.75; N, 3.80.

**Synthesis of Complex (nacnac)Cr(N{CH$_3$}$_2$) (7).** Complex **1** (100 mg, 0.086 mmol) was dissolved in ∼5 mL of ether and cooled to −35 °C. An analogously cooled solution of $LiNMe_2$ (8.68 mg, 0.172 mmol) in ether was added dropwise to the cold solution containing the Cr precursor. The solution color immediately changed to brown upon the addition of the amide and was allowed to stir for 3 h. After the completion of the reaction, the solution was filtered and concentrated to ∼2 mL and stored at −35 °C for 24 h. Brown colored crystals of (nacnac)Cr(N{$CH_3$}$_2$) (**7**) were obtained (76 mg, 0.127 mmol, 75% yield).

For **7**: $^1$H NMR (23 °C, 399.8 MHz, $C_6D_6$) $\delta$ 13.5 ($\Delta\nu_{1/2}$ = 970 Hz), 11.9 ($\Delta\nu_{1/2}$ = 285 Hz), 2.31 ($\Delta\nu_{1/2}$ = 185 Hz); $\mu_{eff}$ = 4.69 $\mu_B$ ($C_6D_6$, 298 K, Evan's method); UV−vis (toluene, 25 °C) 404 ($\epsilon$ = 7902), 385 ($\epsilon$ = 7854), 349 ($\epsilon$ = 6195), and 307 nm ($\epsilon$ = 8303). Compound decomposes over >140 °C. Anal. Calcd for $C_{37}H_{59}N_3Cr$: C, 74.33; H, 9.95; N, 7.03. Found: C, 74.23; H, 9.91; N, 7.03.

**General Parameters for Structural Data Collection and Refinement.** Single crystals of **1** ($Et_2O$), **2**−**5** (pentane), **6** (hexane), and **7** ($Et_2O$) were grown at −35 °C. Inert atmosphere techniques were used to place the crystal onto the tip of a diameter glass capillary (∼0.1 mm) and mounted on a SMART6000 (Bruker) at 117−128(2) K. A preliminary set of cell constants was calculated

(23) (a) Sur, S. K. *J. Magn. Reson.* **1989**, *82*, 169–173. (b) Evans, D. F. *J. Chem. Soc.* **1959**, 2003–2005.
(24) (a) *SAINT 6.1*; Bruker Analytical X-Ray Systems: Madison, WI. (b) *SHELXTL-Plus V5.10*; Bruker Analytical X-Ray Systems: Madison, WI.

from reflections obtained from three nearly orthogonal sets of 20−30 frames. The data collection was carried out using graphite monochromated Mo Kα radiation with a frame time of 2−30 s and a detector distance of 5.0 cm. A randomly oriented region of a sphere in reciprocal space was surveyed. Three sections of 606 frames were collected with 0.30° steps in $\omega$ at different $\phi$ settings with the detector set at −43° in $2\theta$. Final cell constants were calculated from the *xyz* centroids of strong reflections from the actual data collection after integration (SAINT).[24a] The structure was solved using SHELXS-97 and refined with SHELXL-97.[24b] A direct-methods solution was calculated, which provided most non-hydrogen atoms from the E-map. Full-matrix least-squares/difference Fourier cycles were performed, which located the remaining non-hydrogen atoms. All non-hydrogen atoms were refined with anisotropic displacement parameters (unless otherwise mentioned below). All hydrogen atoms were refined with isotropic displacement parameters (unless otherwise mentioned below). The intensity data were corrected for absorption (SADABS).

**Structural Details for Complex 1.** The molecule lies on a two-fold axis. There is also a disordered $Et_2O$ molecule in the cell in addition to the dimer. One of the $^i$Pr groups is also slightly disordered and was modeled using constrained occupancy for the three minor atoms present. All hydrogen atoms with the exception of those associated with the solvent and disorder were located in subsequent Fourier maps and included as isotropic contributors in the final cycles of refinement. The structure was found as proposed with two independent molecules per asymmetric unit.

**Structural Details for Complex 3.** The molecule lies on a crystallographic two-fold axis, which makes the hydrogen atoms associated with the methyl groups disordered. All other hydrogen atoms were located in subsequent Fourier maps and included as isotropic contributors in the final cycles of refinement. The hydrogen atoms associated with the methyl group were placed in ideal positions and refined as riding atoms with relative isotropic displacement parameters.

**Structural Details for Complex 4.** The structure was found as proposed with two independent molecules per asymmetric unit.

**Structural Details for Complexes 5−7.** These structures were found as proposed.

**Theoretical Studies.** All calculations were carried out using Density functional theory as implemented in the Jaguar 6.0 suite.[25] Geometries were optimized with the B3LYP[26] functional and the 6-31G** basis set. For transition metals, the Los Alamos LACVP basis[27] including effective core potentials was used. The energies of the optimized structures were re-evaluated by additional single-point calculations using Dunning's correlation-consistent triple-ζ basis set[28] cc-pVTZ(-f). For transition metals, we used a modified version of LACVP, designated as LACV3P, in which the exponents were decontracted to match the triple-ζ quality basis. Energy decomposition was computed with BP86[29] functional using the Amsterdam density functional (ADF 2006) package,[30] utilizing the triple-ζ basis set (TZP) and the frozen-core approximation. All nonconstrained structures were confirmed to be minima on the potential energy surface by vibrational frequency calculations that showed no imaginary frequency.

## Results and Discussion

**Definition of T-Shaped and Y-Shaped Structures.** To quantify the extent of distortion from a perfect Y- or T-shape, we introduce the "tee" value, defined by difference between the two N−Cr−X angles and dividing the quantity by 90°. This parameter ranges from 0 to 1 for the change of perfect Y-shaped structure to ideal T-shaped structure. Since the ligand used in the present work is very sterically demanding, attainment of the ideal T-shaped structure seems quite unreasonable. Such structures with deviation from ideal T-shape are characterized as a distorted T-shaped structure where the tee value becomes significantly larger than 0; we chose the value larger than 0.1 as a characteristic criterion.

***Scheme 1***

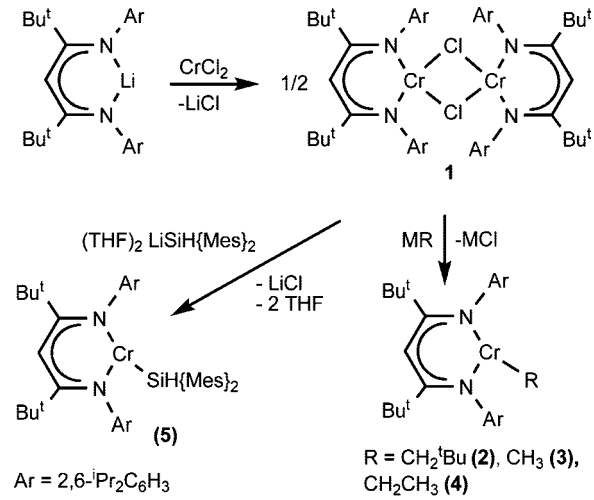


**Synthesis of the Cr(II) β-Diketiminate Precursor.** When Li(nacnac) was added to $CrCl_3(THF)_3$ in cold THF (−35 °C), the dimer $[(nacnac)Cr(\mu\text{-}Cl)]_2$ (**1**) was isolated only in poor yield along with traces of the free β-diketimine base $[ArNC(^tBu)]_2CH_2$, which we attribute to the redox activity of Cr(III) leading to undesirable side reactions. Consequently, we attempted to access **1** by direct transmetalation of anhydrous $CrCl_2$ with Li(nacnac) and were able to isolate the desired product in moderate yield (53%) from THF (Scheme 1). Gibson and coworkers[2b] also applied this strategy for the synthesis of an analogous dimer system using a less hindering β-diketiminate ligand, $[ArNC(CH_3)]_2CH^-$.[31] Complex **1** was characterized by a combination of physical methods including Evans ($\mu_{eff} = 2.95$ $\mu_B$ per Cr center), elemental analysis, and single-crystal X-ray diffraction studies. The low-spin magnetic moment of **1** in solution suggests antiferromagnetic coupling mediated through the $[Cr(\mu\text{-}Cl)]_2$ core, while single-crystal structural analysis reveals the correct connectivity and degree of aggregation (Figure 1). Complex **1** is isostructural to Gibson's $\{([ArNC(CH_3)]_2CH)Cr(\mu\text{-}Cl)\}_2$ but resistant to solvation to form a hypothetical adduct such as $[(nacnac)Cr(\mu\text{-}Cl)(THF)]_2$.[2] Hence, the $^t$Bu groups in the β-carbon position provide sufficient steric bulk to prevent Lewis base adduct from coordinating strongly (if any). In addition, these sterically demanding substituents push the flanking aryl groups closer to the metal center, thus disfavoring strong Cr−Cr interactions and ligand disproportionation to form bis-β-diketiminate chromous systems that are often observed for the parent N−Ph derivative[32] exploited by Theopold.[1c] As anticipated for an unsaturated three-coordinate Cr(II) compound

(25) *Jaguar*, 6.0 ed.; Schrödinger, L.L.C.: Portland, OR, 1991−2005.
(26) (a) Becke, A. D. *J. Chem. Phys.* **1993**, *98*, 5648–5652. (b) Lee, C. T.; Yang, W. T.; Parr, R. G. *Phys. Rev. B* **1988**, *37*, 785–789.
(27) Hay, P. J.; Wadt, W. R. *J. Chem. Phys.* **1985**, *82*, 270–283.
(28) Dunning, T. H. *J. Chem. Phys.* **1989**, *90*, 1007–1023.
(29) (a) Becke, A. D. *Phys. Rev. A* **1988**, *38*, 3098–3100. (b) Perdew, J. P.; Wang, Y. *Phys. Rev. B* **1986**, *33*, 8800–8802.
(30) te Velde, G. T.; Bickelhaupt, F. M.; Baerends, E. J.; Guerra, C. F.; Van Gisbergen, S. J. A.; Snijders, J. G.; Ziegler, T. *J. Comput. Chem.* **2001**, *22*, 931–967.
(31) Stender, M.; Wright, R. J.; Eichler, B. E.; Prust, J.; Olmstead, M. M.; Roesky, H. B.; Power, P. P. *Dalton Trans.* **2001**, 3465–3469.
(32) Budzelaar, P. H.; de Gelder, R.; Gal, A. W. *Organometallics* **1998**, *17*, 4121–4123.

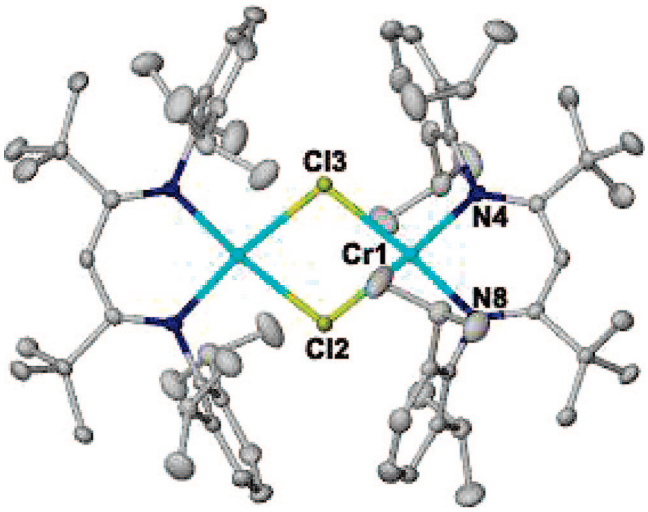


***Figure 1.*** Molecular structure of complex **1** depicting thermal ellipsoids at the 50% probability level. Hydrogen atoms and one $Et_2O$ molecule have been excluded for clarity. Distances are reported in angstroms and angles in degrees, and crystal data are listed in Table 1. Selected metrical parameters: Cr1−N4, 2.059(3); Cr1−N8, 2.063(3); Cr1−Cl2, 2.4182(4); Cr1−Cl3, 2.4316(4); N4−Cr1−N8, 90.69(5); N4−Cr1−Cl2, 168.03(4); N8−Cr1−Cl2, 95.98(4); N4−Cr1−Cl3, 97.45(4); N8−Cr1−Cl3, 167.85(4); Cl2−Cr1−Cl3, 77.66(7). Crystallographic data are reported in Table 1.

having a donor group (e.g., $Cl^-$), each Cr center in complex **1** resides in a square-planar coordination environment due to bridging of the $Cl^-$ ligands. The steric hindrance imposed by the nacnac$^-$ ligand is partially reflected by the less obtuse $C_{ipso}$−N−Cr angles of 111.14 and 111.31° for **1** versus 116.94 and 118.89° along with $C_\beta$−N−$C_{ipso}$ angle of 122.20 versus 116.27° for Gibson's complex $\{([ArNC(CH_3)]_2CH)Cr(\mu\text{-}Cl)\}_2$.[2] Likewise, the Cr···Cr distance is much greater in **1** (3.7780(6) Å) versus ~3.60 Å for $[([ArNC(CH_3)]_2CH)Cr(\mu\text{-}Cl)]_2$,[2] which may be a result of the steric demands of the $^t$Bu groups.

**Synthesis of Neutral, Three-Coordinate Cr(II) Complexes with a *σ*-Donor Ligand.** With complex **1** being sterically protected and the Cr−Cl bond length being longer than usual (2.41−2.43 Å vs 2.39 Å for complex $\{([ArNC(CH_3)]_2CH)Cr(\mu\text{-}Cl)\}_2$,[2] we envisioned that substitution of the chloride by a functional group that is less prone to serve as a bridging ligand may give access to stable monomeric three-coordinate chromium(II) complexes. Analogous high-spin, three-coordinate Fe(II)-alkyl species were previously isolated from the reaction of (nacnac)FeCl and alkyl reagents,[33] but three-coordinate chromous complexes are exceedingly rare.[34] Gratifyingly, treatment of **1** with 2 equiv of $LiCH_2{}^t$Bu afforded yellow crystals of the monomer (nacnac)Cr($CH_2{}^t$Bu) (**2**) in 51% yield (Scheme 1). Complex **2** is in a high spin state with a $\mu_{eff} = 5.09\ \mu_B$ and displays a distorted T-shaped coordination geometry (tee = 0.447), as confirmed by single-crystal X-ray diffraction measurements (Figure 2). The chromium center is essentially planar

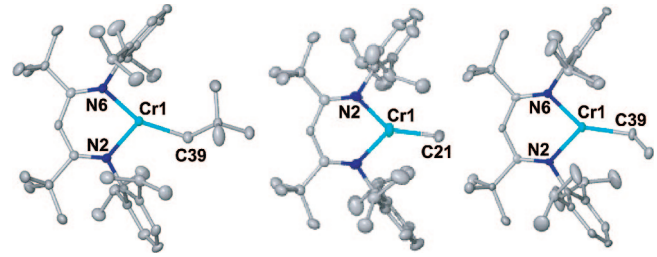


***Figure 2.*** Molecular structures of complexes **2** (left), **3** (center), and **4** (right) depicting thermal ellipsoids at the 50% probability level and with H-atoms excluded for clarity. Distances are reported in Table 2, and crystal data are listed in Table 1.

with a slight dislocation of Cr from the NNC plane of only 0.126 Å and exhibits a distorted T-shaped geometry (N−Cr−N, 90.93(5) Å; N−Cr−$C_\alpha$, 153.91(7) Å; N−Cr−$C_\alpha$, 113.67(7) Å, Table 2). Location and isotropic refinement of hydrogen atoms in the Fourier map of **2** do not suggest α- or *γ*-agostic hydrogen interactions in the solid state structure. Another salient feature in the molecular structure of **2** is the Cr−$C_\alpha$ bond length of 2.139(9) Å, which is considerably longer than Cr−C bonds found in the more common Cr(III) alkyl complexes that typically span a range of ~2.04−2.09 Å,[1,2] therefore hinting that the Cr-alkyl moiety in **2** may display interesting chemical reactivity. The computed Cr−C distance in **2** is notably shorter than observed experimentally in Theopold's asymmetric Cr(II) dimer $[([ArNC(CH_3)]_2CH)Cr]_2(\mu_2\text{-}H)(\mu_2\text{-}CH_2SiMe_3)$ (Cr1−C, 2.29 Å and Cr2−C, 2.19 Å).[5b]

The steric demand of the alkyl group and absence of *β*-hydrogens do not appear to control the formation or to impact the stability of the three-coordinate monomer **2** inasmuch as treatment of **1** with 2 equiv of MeMgCl or EtMgCl affords the methyl and ethyl analogues (nacnac)Cr(R) (R = $CH_3$, **3**; R = $CH_2CH_3$, **4**) in 53 and 57% yield, respectively, following recrystallization of the mixture from pentane at −35 °C (Scheme 1). Holland has previously studied similar three-coordinate ferrous alkyls supported by sterically encumbering *β*-diketiminate ligands.[33] The moderate yield for the isolation of **3** and **4** reflects on their lipophilic nature leading to high solubility in most common organic solvents. As seen for **2**, complexes **3** and **4** are also thermally stable and display solution magnetic data consistent with a high-spin $d^4$ Cr(II) center ($\mu_{eff} = 5.06\ \mu_B$, **3**; $\mu_{eff} = 4.89\ \mu_B$, **4**). Single-crystal X-ray diffraction analysis exposes a monomeric composition for both complexes, as shown in Figure 2, and the geometry does not seem to be sensitive to the steric demands of the alkyl group. For instance, in complex **4**, the alkyl ligand is unsymmetrically disposed with respect to the nacnac$^-$ ligand with a Cr−$C_\alpha$ bond displaced from the N−Cr−N bisector, while the deviation of the methyl group in complex **3** is notably smaller (the angles are different for N2−Cr1−C21, 142.03(13)°, and N2′−Cr1-C21, 126.89(13)°). Although the degree of distortion from the ideal Y-shaped coordination geometry is slightly different, it is fair to generalize that all alkyl ligands give rise to T-shaped coordination geometries.

Other salient structural features for complexes **3** and **4** include long Cr−$C_{alkyl}$ bond lengths 2.081(3) (**3**) and 2.118(5) Å (**4**) and planar Cr centers (displacement of Cr atoms from the NNC plane is negligible at ~0.027−0.00 Å). The absence of α- or *β*-hydrogen agostic interactions in **3** or **4** constitutes a stark contrast to electronically unsaturated, three-coordinate Ni(II)−ethyl complexes bearing sterically demanding *β*-diketiminate ligands.[35] For all alkyls, the UV−vis spectra in $C_6H_6$ display

(33) (a) Smith, J. M.; Lachicotte, R. J.; Holland, P. L. *Organometallics* **2002**, *21*, 4808–4814. (b) Vela, J.; Vaddadi, S.; Cundari, T. R.; Smith, J. M.; Gregory, E. A.; Lachicotte, R. J.; Flaschenriem, C. J.; Holland, P. L. *Organometallics* **2004**, *23*, 5226–5239.

(34) Three-coordinate "ate" complexes of Cr(II) have been scarcely reported: (a) Sydora, O. L.; Wolczanski, P. T.; Lobkovsky, E. B.; Buda, C.; Cundari, T. R. *Inorg. Chem.* **2005**, *44*, 2606–2618. (b) Hvoslef, J.; Hope, H.; Murray, B. D.; Power, P. P. *J. Chem. Soc., Chem. Commun.* **1983**, 1438–1439.

(35) Kogut, E.; Zeller, A.; Warren, T. H.; Strassner, T. *J. Am. Chem. Soc.* **2004**, *126*, 11984–11994.

***Table 1.*** Crystallographic Data for Complexes **2**−**4**

| complex | 1·$Et_2O$ | 2 | 3 | 4 |
|---|---|---|---|---|
| empirical formula | $C_{74}H_{116}Cl_2Cr_2N_4O$ | $C_{40}H_{64}CrN_2$ | $C_{36}H_{56}CrN_2$ | $C_{37}H_{58}CrN_2$ |
| fw | 1252.61 | 624.93 | 568.83 | 582.85 |
| crystal system | monoclinic | monoclinic | monoclinic | monoclinic |
| space group | *C*2/*c* | *P*2(1)/*n* | *C*2/*c* | *P*2(1)/*n* |
| *a* (Å) | 21.3016(16) | 9.9035(7) | 16.8123(15) | 24.296(3) |
| *b* (Å) | 21.5950(18) | 17.6060(12) | 9.5254(8) | 18.010(2) |
| *c* (Å) | 15.8181(13) | 21.5766(16) | 22.6128(19) | 16.7470(19) |
| α (°) | | | | |
| *β* (°) | 99.408(2) | 97.806(2) | 108.231(2) | 109.941(4) |
| *γ* (°) | | | | |
| *V* (Å$^3$) | 7178.6(10) | 3727.3(5) | 3439.5(5) | 6888.7(14) |
| *Z* | 4 | 4 | 4 | 8 |
| $D_{calcd}$(g·cm$^{-3}$) | 1.159 | 1.114 | 1.098 | 1.124 |
| crystal size (mm) | 0.25 × 0.25 × 0.18 | 0.30 × 0.30 × 0.30 | 0.35 × 0.35 × 0.18 | 0.18 × 0.15 × 0.04 |
| solvent | $Et_2O$ | pentane | pentane | pentane |
| color | forest green | yellow-green | yellow-green | yellow |
| (*h*, *k*, *l*) | $-27 \le h \le 27$, $-28 \le k \le 28$, $-20 \le l \le 20$ | $-12 \le h \le 12$, $-22 \le k \le 22$, $-28 \le l \le 28$ | $-21 \le h \le 21$, $-12 \le k \le 12$, $-29 \le l \le 29$ | $-37 \le h \le 33$, $-27 \le k \le 27$, $-25 \le 1\,' 17$ |
| *F*(000) | 2712 | 1368 | 1240 | 2544 |
| Θ range | 1.89−27.53 | 1.91−27.52 | 2.49−27.53 | 2.11−33.22 |
| linear abs. coeff. (mm$^{-1}$) | 0.421 | 0.335 | 0.357 | 0.358 |
| total reflns collected | 81142 | 32011 | 37751 | 74308 |
| independent reflns | 8274 | 8572 | 3972 | 25656 |
| unique reflns | 5651 | 5459 | 2610 | 4984 |
| $R_{int}$ | 0.0699 | 0.0629 | 0.0891 | 0.3072 |
| data/parameter | 8274/631 | 7503/644 | 3956/285 | 25656/760 |
| $R_1$, $wR_2$ (for $I > 2\sigma(I)$ | 0.0340, 0.0903 | 0.0370, 0.0819 | 0.0406, 0.0810 | 0.0669, 0.1473 |
| GoF | 0.946 | 0.884 | 1.193 | 0.642 |
| peak/hole (e/Å$^{-3}$) | 0.637/−0.348 | 0.319/−0.327 | 0.403/−0.307 | 0.383 /−0.383 |

two diagnostic charge transfer (CT) bands of medium intensity and centered at 386 and 404 nm ($\epsilon$ = 2753 and 3104 M$^{-1}$ cm$^{-1}$, **2**), 305 and 403 nm ($\epsilon$ = 3823 and 3358 M$^{-1}$ cm$^{-1}$, **3**), and 405 and 421 nm ($\epsilon$ = 3214 and 2953 M$^{-1}$ cm$^{-1}$, **4**). The $\epsilon$ values are in sharp contrast to larger values observed for square planar Cr(II) systems such as **1** ($\epsilon$ = 6963 at 386 nm and $\epsilon$ = 10767 at 405 nm).

In addition to alkyls, other strong $\sigma$-donors can apparently encourage T-shape geometry. When **1** is treated with 2 equiv of the silyl anion (THF)$_2$LiSiH{2,4,6-$Me_3C_6H_2$}$_2$, the Cr(II) silyl complex (nacnac)Cr(SiH{2,4,6-$Me_3C_6H_2$}$_2$) (**5**) is readily formed as a yellow material (Scheme 1). Magnetic susceptibility data for **5** are in accord with a high-spin chromous complex ($\mu_{eff}$ = 4.71 $\mu_B$), and the solid state structure clearly depicts a three-coordinate Cr(II) system bearing the terminal silyl moiety (Cr−Si, 2.6603(8) Å, Figure 3), which to our surprise represents the first crystallographically characterized Cr−silyl complex. Selected metrical parameters for **5** are listed in Table 2, and crystallographic data are given in Table 3. In the structure of **5**, the Cr atom resides essentially in the imaginary plane defined by its first coordination sphere of atoms N−Si−N (∼0.013 Å). However, the most notable structural feature in **5** is the deviation of the silyl group from a strict Y-shape geometry to adopt the T-shape coordination geometry (tee = 0.375). This observation is best represented by the asymmetry in the $N_{nacnac}$−Cr−$Si_\alpha$ angles 152.12(6) and 118.40(6)° (Table 2). Despite the hydrogen on the silyl atom being located in subsequent Fourier maps and included as isotropic contributors in the final cycles of refinement as well as refined isotropically, the pyramidalization at Si coupled with the magnetization further corroborates our claims for this species having a high-spin Cr(II) center bearing a secondary silyl group.

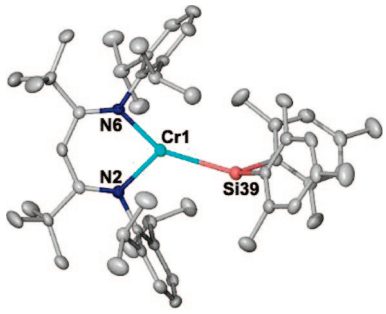


***Figure 3.*** Molecular structures of complex **5** depicting thermal ellipsoids at the 50% probability level and with H-atoms excluded for clarity. Selected distances are reported in Table 2, and crystal data are listed in Table 3.

**Synthesis of Neutral, Three-Coordinate Cr(II) with Strong *π*-Donor Ligands.** To probe for how the electronic nature of the third ligand influences the geometry in these chromous complexes, we explored salt metathesis chemistry in **1** with alkoxide ligands. When **1** is treated with NaO{2,6-$^i$Pr$_2$C$_6$H$_3$} in THF, the alkoxide complex (nacnac)Cr(O{2,6-$^i$Pr$_2$C$_6$H$_3$}) (**6**) is isolated in 42% yield as a yellow colored crystal (Scheme 2). Not surprisingly, solution magnetization data at 25 °C are in accord with complex **6** having a high-spin Cr(II) system ($\mu_{eff}$ = 4.77 $\mu_B$). To our surprise, however, the solid state structure of **6** displayed a monomeric Cr(II) alkoxide (Cr−O, 1.872(2) Å) complex with a Y-shape planar geometry (tee = 0.003), whereby the aryl residue on the alkoxide is almost oriented parallel with respect to the (nacnac)Cr plane (Figure 4). Salient features for Y-shape coordination in **6** is reflected by the nearly identical N−Cr−O angles of 134.88(8) and 134.62(8)° (Table 2). The Cr−O distance is comparable to other low-coordinate Cr(II) alkoxide ligands reported in the literature.[34] One may anticipate a dominating role of sterics in **6** given that a Y-geometry is preferred. However, the orientation and near planarity of the aryloxide group (17.5° deviation of the $OCC_{ortho}$

***Table 2.*** Selected Metrical Parameters for the Structures of Complexes **2**−**7** where $X^-$ Represents $CH_2{}^tBu$ (**2**), $CH_3$ (**3**), $CH_2CH_3$ (**4**), $SiH\{2,4,6\text{-}Me_3C_6H_2\}_2$ (**5**), $O\{2,6\text{-}{}^iPr_2C_6H_3\}$ (**6**), $N\{CH_3\}_2$ (**7**), and N Represents the $\beta$-Diketiminate $\alpha$-Nitrogen (Distances are Reported in Angstroms and Angles in Degrees)

| complex | **2** | **3** | **4** | **5** | **6** | **7** |
|---|---|---|---|---|---|---|
| Cr−N | 1.9981(14) | 1.9785(14) | 1.996(3) | 1.9906(19) | 1.991(2) | 1.9923(11) |
| Cr−N | 2.0074(13) | 1.9785(14) | 1.998(3) | 2.0090(19) | 1.993(2) | 2.0094(11) |
| Cr−X | 2.1386(19) | 2.097(3) | 2.118(5) | 2.6603(8) | 1.872(2) | 1.9511(12) |
| N−Cr−N | 90.93(5) | 91.05(8) | 90.98(13) | 89.46(8) | 90.46(9) | 91.59(4) |
| N−Cr−X | 153.91(7) | 142.03(13) | 143.6(2) | 152.12(6) | 134.88(8) | 136.27(8) |
| N−Cr−X | 113.67(7) | 126.89(13) | 125.3(2) | 118.40(6) | 134.62(8) | 132.90(8) |
| Cr displacement from the imaginary NNX plain | 0.13 | 0.00 | 0.03 | 0.01 | 0.02 | 0.00 |
| tee | 0.447 | 0.168 | 0.203 | 0.375 | 0.003 | 0.037 |

***Table 3.*** Crystallographic Data for Complexes **5**−**7**

| complex | **5** | **6** | **7** |
|---|---|---|---|
| empirical formula | $C_{53}H_{76}CrN_2Si$ | $C_{47}H_{70}CrN_2O$ | $C_{37}H_{59}CrN_3$ |
| fw | 821.25 | 731.05 | 597.87 |
| crystal system | orthorhombic | triclinic | monoclinic |
| space group | *Pbcn* | $P\bar{1}$ | $P2(1)/n$ |
| *a* (Å) | 34.221(3) | 10.0616(11) | 9.7282(7) |
| *b* (Å) | 13.3963(12) | 10.1069(11) | 17.3211(11) |
| *c* (Å) | 21.1992(19) | 21.264(2) | 21.3090(14) |
| α (°) | 90 | 91.477(3) | |
| *β* (°) | 90 | 93.136(3) | 95.8084(12) |
| *γ* (°) | 90 | 94.606(3) | |
| *V* (Å$^3$) | 9718.5(15) | 2151.2(4) | 3572.2(4) |
| *Z* | 8 | 2 | 4 |
| $D_{calc}$(g•cm$^{-3}$) | 1.123 | 1.129 | 1.112 |
| crystal size (mm) | 0.35 × 0.30 × 0.13 | 0.25 × 0.25 × 0.20 | 0.22 × 0.20 × 0.18 |
| solvent, color | pentane, yellow-green | hexane, red/blue/brown | ether, dichroic brown-blue |
| (*h*, *k*, *l*) | $-44 \le h \le 44$, $-17 \le k \le 16$, $-26 \le l \le 27$ | $-13 \le h \le 13$, $-11 \le k \le 13$, $-27 \le l \le 27$ | $-12 \le h' 12$, $-22 \le k' 12$, $-27 \le l \le 27$ |
| *F*(000) | 3568 | 796 | 1304 |
| Θ range | 2.01−27.53 | 2.02−27.53 | 1.52−27.52 |
| linear abs. coeff. (mm$^{-1}$) | 0.295 | 0.301 | 0.347 |
| total reflns collected | 98958 | 18933 | 33359 |
| independent reflns | 11182 | 9854 | 8229 |
| unique reflns | 5305 | 5519 | 6396 |
| $R_{int}$ | 0.1540 | 0.0948 | 0.0359 |
| data/parameter | 13875 /818 | 9743/718 | 8229/386 |
| $R_1$, $wR_2$ (for $I > 2\sigma(I)$) | 0.0427, 0.0923 | 0.0552, 0.1273 | 0.0511, 0.1649 |
| GoF | 0.804 | 0.843 | 1.067 |
| peak/hole (e/Å$^{-3}$) | 0.433/−0.457 | 0.691/−0.514 | 0.471/−0.919 |

plane with respect to the N−Cr−N bisector plane) can be seen as an indication that electronic elements are more important in this type of geometry versus the T-shape geometry observed for the alkyl and silyl analogues **2**−**5**.

On the basis of our above hypothesis, we questioned whether a small $\pi$-donor ligands would still facilitate Y-shape assembly in a Cr(II) complex. The treatment of **1** with 2 equiv of $LiN\{CH_3\}_2$ in ether resulted in an immediate color change to brown, and subsequent workup of the reaction mixture afforded brown crystals of the dimethylamide chromous derivative (nacnac)Cr($N\{CH_3\}_2$) (**7**) in 75% yield. Solution Evans magnetization measurements were consistent with a high-spin Cr(II) monomer, thus affording a $\mu_{eff} = 4.69\ \mu_B$. In order to unambiguously confirm the degree of aggregation as well as the exact coordination about the Cr(II) ion, we relied on single-crystal X-ray diffraction analysis. As depicted in Figure 4, the molecular structure in a single crystal of compound **7** is akin to that of **6**, whereby the dimethylamide moiety is planar and the geometry at the Cr(II) center is Y-shaped, thence clearly suggesting that electronic features dominate this type of geometry for $\pi$-donor ligands. Metrical parameters for Y-shape coordination in **7** are reflected by the nearly identical N−Cr−N angles of 136.27(8) and 132.90(8)° (Table 2). The only significant change is the greater skewing of the dimethylamide imaginary plane oriented 51.4° with respect to the (nacnac)Cr imaginary plane. As anticipated for a better $\pi$-donor, the Cr−$N\{CH_3\}_2$ distance is slightly shorter than the Cr−$N_{nacnac}$ distances (Table 2).

***Scheme 2.*** Synthesis of Compounds **6** and **7** from Precursor **1**

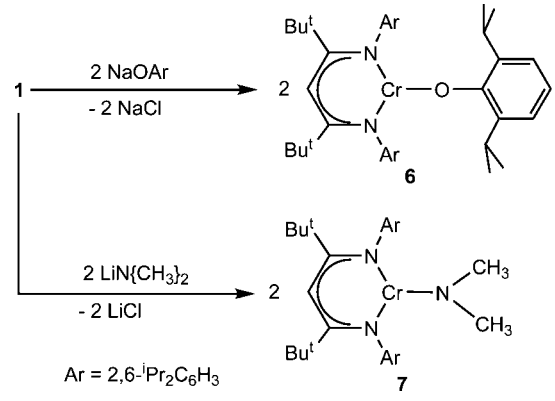

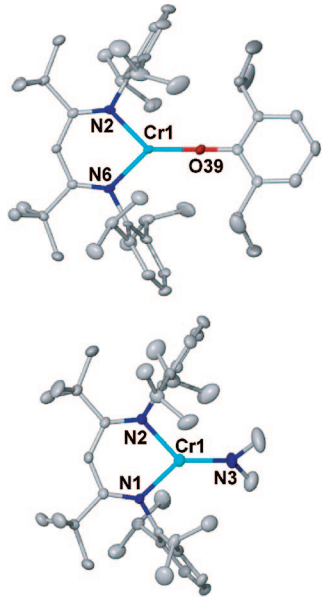


***Figure 4.*** Molecular structure of complexes **6** (top) and **7** (bottom) depicting thermal ellipsoids at the 50% probability level with H-atoms excluded for clarity. Selected distances are reported in Table 2 and crystal data are listed in Table 3.

**Theoretical Analysis of Three-Coordinate Cr(II) Complexes.** To better understand the electronic features that determine the observed coordination geometry for our list of neutral, three-coordinate chromous systems, we conducted a series of computational studies using density functional theory. Using the full ligand set, our calculations show fair agreement with the experimental observations that the T-shaped structure is energetically slightly more favorable than Y-shaped for the methyl complex by 0.32 kcal/mol, which is too small of an energy difference to make a definitive judgment, whereas the Y-shaped coordination geometry is clearly preferred for the aryloxy complex over the T-shaped structure by 4.66 kcal/mol (for the methyl complex, the T-shaped structure is a minimum and the Y-shaped structure is a constrained structure, and vice versa for the aryloxy complex). Interestingly, this relative energy ordering pattern is maintained and a bit amplified when the nacnac ligand is drastically simplified to its barebone skeleton, denoted as nacnac′ (nacnac′ = $^{-}$[HNCH]$_2$CH), and the aryloxy group is simplified to a methoxy ligand (Figure 5), suggesting that the sterically bulky decoration of the nacnac ligand and the aryl moiety of the oxygen-donor ligand have only a small effect on the relative stability of the different structures, whereas there appears to be a fundamental, qualitative reason for pure $\sigma$-donors preferring T- and $\pi$-donors enforcing Y-shaped geometries. The simplified T-shaped model complex **3a** is 1.71 kcal/mol lower in energy than the Y-shaped analogue **3b**, whereas the Y-shaped methoxy structure **8b** is calculated to be 1.71 kcal/mol lower in energy than its T-shaped analogue **8b** (Figure 5). The identical amount of energy that these model complexes differ by is purely accidental. If the nacnac′ backbone is frozen at the structure found in **3a** and the methyl ligand is forced to adopt the Y-shaped structure to afford **3b′**, we obtain an energy difference of 2.8 kcal/mol. Interestingly, the opposite trend is observed for the methoxy system. Distorting the Y-shaped geometry of **8b** to a T-shaped analogue while keeping the nacnac′ fixed to afford **8a′** is energetically uphill by 3.2 kcal/mol. The energy drops to −3.2 kcal/mol compared to **8a**. These energies again suggest that there is a fundamental

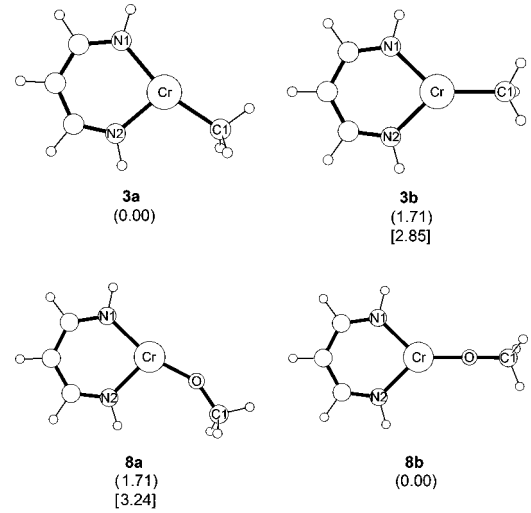


***Figure 5.*** Computed structures and relative energies of simplified model complexes. Relative energies of the fully optimized structures are given in kcal/mol in parenthesis. Relative energies computed by keeping the (nacnac′)Cr fragment fixed at the geometry found in the lower energy structure and enforcing the high-energy Cr structure are given in square brackets.

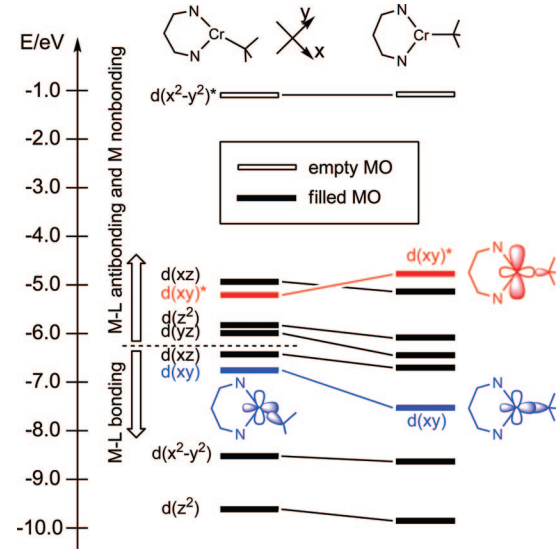


***Figure 6.*** Walsh diagram of the (nacnac′)Cr(CH$_3$) complex varying the geometry from T → Y.

electronic reason for the preference of the T-shaped geometry for the alkyl ligand, while the Y-shaped coordination geometry is energetically lower for the alkoxy ligand.

Walsh diagrams that relate MO energies to structural change are the most obvious ways of analyzing the electronic differences between two structural isomers. Figure 6 shows the Walsh diagram comparing the most salient electronic features of **3a** with those of **3b′**. Consistent with a Cr(II)−d$^4$ system, we found four singly occupied, mostly metal-based frontier MOs that are M−L nonbonding or antibonding in character. The M−L bonding MOs that are doubly occupied are also located and shown in Figure 6. The MOs that are most affected by the structural change T → Y are not surprisingly the Cr−d(*xy*)-based MOs. In **3a**, the M−L bonding interaction between Cr−d(*xy*) and the methyl sp orbitals is weak because the orbital overlap is poor, as illustrated in blue in Figure 6. The Y-shaped coordination geometry is much more favorable for this interac-

***Table 4.*** Computed Component (BP86/TZP) for the Interaction between (nacnac′)Cr and $CH_3/OCH_3$ in T-Shape and Y-Shape (nacnac′)Cr($CH_3/OCH_3$)

| | (nacnac′)Cr($CH_3$) | | | (nacnac′)Cr($OCH_3$) | | |
|---|---|---|---|---|---|---|
| (in kcal/mol) | T-shaped | Y-shaped | Δ | T-shaped | Y-shaped | Δ |
| Pauli repulsion (PR) | 158.29 | 167.75 | 9.46 | 112.17 | 130.15 | 17.98 |
| electrostatic interaction (EI) | −281.95 | −285.94 | −3.99 | −203.23 | −211.48 | −8.25 |
| non-orbital interaction (PR+EI) | −123.67 | −118.19 | 5.48 | −90.06 | −81.33 | 8.73 |
| orbital interaction | −154.58 | −157.21 | −2.63 | −184.44 | −196.41 | −11.97 |
| total energy | −278.25 | −275.40 | 2.85 | −274.50 | −277.74 | −3.24 |
| total energy (B3LYP) | | | 1.71 | | | −1.71 |

tion, and the MO energy decreases significantly from −6.92 to −7.66 eV, as illustrated in Figure 6 (shown in blue). The corresponding M−L antibonding interaction, labeled as d($xy$)*, is of course unfavorable energetically, and the MO energy increases from −5.42 to −5.00 eV (red in Figure 6). Interestingly, there is notable mixing of Cr 4s orbital character in this MO, which decreases the size of the orbital lobe that points directly to the methyl ligand and dampens the unfavorable antibonding interaction. As a result, the stabilization of the d($xy$) orbital is more pronounced than the destabilization of the d($xy$)* orbital, as the Walsh diagram illustrates clearly. This observation is counterintuitive, as this electronic structure pattern would give preference to the Y-shaped structure energetically. Interestingly, the other occupied MOs are also lowered energetically during the T → Y transformation. The only plausible conclusion from this analysis is that the purely orbital-based electronic component of the total energy prefers the Y-shaped coordination geometry for the methyl complex.

Table 4 enumerates the components of the total energy derived following the Ziegler−Rauk decomposition scheme,[36] where the (nacnac′)Cr skeleton is kept fixed and the methyl group is moved from the T- to Y-position. In good agreement with the discussion presented above, the orbital interaction energy of the Y-shaped Cr−methyl complex is −157.2 compared to −154.6 kcal/mol in the T-shaped complex, indicating that, on the basis of orbital interactions only, the Y-shaped geometry is favored by 2.6 kcal/mol over the T-shaped alternative. The non-orbital interaction overrides this preference, however, and our calculations quantify that preference to be 5.5 kcal/mol in favor of the T-shaped geometry, to afford the overall preference of 2.8 kcal/mol for the T-shaped coordination geometry. In other words, the T-shaped coordination geometry is energetically preferred because it allows for minimizing the Pauli repulsion between the methyl group and the (nacnac′)Cr moiety. Interestingly, a similar trend is observed for the methoxy complex (nacnac′)Cr($OCH_3$). The Y-shaped coordination geometry gives an orbital interaction energy of −196.4 compared to −184.4 kcal/mol in the T-shaped geometry, whereas the non-orbital component is in favor of the T-shaped geometry by 8.7 kcal/mol. As a result, the Y-shaped geometry is 3.2 kcal/mol lower in energy than the T-shaped geometry. In conclusion, these observations suggest that very similar forces are at play for both methyl and methoxy complexes, generally favoring the Y-shaped geometry for orbital interaction reasons, while giving preference to the T-shaped geometry for non-orbital interaction terms. The methyl complex adopts T-shaped geometry because the differential orbital interaction energy of −2.6 kcal/mol is not large enough to overwrite the non-orbital component, whereas the methoxy complex adopts Y-shaped geometry because the differential orbital interaction energy of 12.0 kcal/mol is large enough to overcome an intrinsic energy penalty associated with the Y-shaped coordination geometry.

The scheme in Figure 7 gives a conceptual summary of the electronic features leading to the energy trends found in our calculations. As discussed previously, the nacnac framework establishes the relative ordering of the frontier orbitals and enforces the d($x^2-y^2$) dominated orbital to be the LUMO of the $d^4$ high-spin system, while the d($xy$) dominated MO is occupied by one electron. For understanding the non-orbital interactions, it is important to recognize that orbital mixing between the fragments cannot be considered, as it is captured in the orbital interaction portion of the total energy. Instead, we must concentrate on Pauli repulsions that emerge as the result of electron clouds from the fragments spatially penetrating each other. Thus, structures will display favorable non-orbital interaction energies when occupied orbitals of the fragments show little overlap with each other. Placing the $\sigma$-donor ligands at a position to give the Y-shaped coordination geometry leads to significant spatial overlap with the half-filled d($xy$) orbital, as illustrated in Figure 7a. At the ligand position in the T-shaped geometry, however, this interaction is avoided and the $\sigma$-donor orbital is aligned with the empty d($x^2-y^2$) orbital of the metal. In other words, the metal fragment electron density at the Y-position is higher than that at the T-position because the d($x^2-y^2$) orbital is empty and the d($xy$) orbital is filled, and placing any Lewis base at the Y-ligand position will lead to higher overlap between the metal and Lewis base electron densities, which in turn gives rise to higher Pauli repulsion terms for the Y-shaped coordination geometry. The magnitude of preference for the T-shaped geometry from non-orbital interactions only is comparable in both structures, with energy differences being 5.5 and 8.7 kcal/mol for the methyl and methoxy complexes, respectively. This finding is in good agreement with the rationale discussed above, as one would not expect much variation of the interaction patterns in the non-orbital subspace where only the occupied orbitals of the two fragments are allowed to interact with each other. This interaction pattern will be present in all formally anionic $\sigma$-donor ligands.

The obvious difference between the two ligands in the simplified models (nacnac′)Cr($CH_3$) and (nacnac′)Cr($OCH_3$) is that the methoxy ligand can act as a $\pi$-base. As four of the five Cr−d-dominated fragment orbitals are half-occupied, only the d($x^2-y^2$)-dominated empty MO is the ideal $\pi$-accepting orbital,

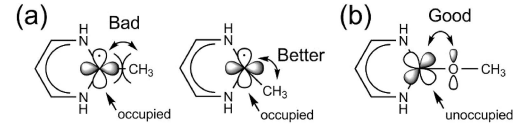


***Figure 7.*** Conceptual summary of the interactions leading to the observed trends in the energy components.

(36) (a) Ziegler, T.; Rauk, A. *Inorg. Chem.* **1979**, *18*, 1755–1759. (b) Frenking, G.; Fröhlich, N. *Chem. Rev.* **2000**, *100*, 717–774.

***Table 5.*** Computed Component for the Interaction between (nacnac′)Sc and $CH_3/OCH_3$ in T-Shape and Y-Shape (nacnac′)Sc($CH_3/OCH_3$)

| | (nacnac′)Sc($CH_3$) | | | (nacnac′)Sc($OCH_3$) | | |
|---|---|---|---|---|---|---|
| (in kcal/mol) | T-shaped | Y-shaped | Δ | T-shaped | Y-shaped | Δ |
| Pauli repulsion (PR) | 133.26 | 130.21 | −3.05 | 94.66 | 89.46 | −5.20 |
| electrostatic interaction (EI) | −262.14 | −264.10 | −1.96 | −207.27 | −208.53 | −1.26 |
| non-orbital interaction (PR+EI) | −128.88 | −133.89 | −5.01 | −113.20 | −119.07 | −5.87 |
| orbital interaction | −64.34 | −66.59 | −2.25 | −96.03 | −94.30 | 1.73 |
| total energy | −193.22 | −200.48 | −7.26 | −209.24 | −213.37 | −4.13 |

which requires the methoxy ligand to be placed in the Y-shaped coordination geometry. In the T-shaped geometry, a M−L $\pi$-bonding orbital is formed between the d($xy$) and the oxygen p-orbitals, and we were able to locate it at −6.95 eV, but the out-of-phase combination $\pi$*-orbital is also occupied by one electron. These MOs are labeled as d($xy$) and d($xy$)*, respectively, and are highlighted in blue in Figure 8. Upon moving the methoxy ligand to the position affording the Y-shaped coordination geometry, the O p-orbital can form a doubly occupied $\pi$-bond orbital with the d($x^2-y^2$) MO, while leaving the $\pi$*-orbital empty, as indicated by the red line in Figure 8 and conceptualized in Figure 7b. The d($xy$)-dominated MO becomes nonbonding in the Y-shaped geometry. Given these easily comprehensible electronic structure changes, we expect a significant energetic consequence in the orbital interaction component of the total energy, and our calculations quantify it to be 12.0 kcal/mol (Table 4), which is more than four times larger than the differential orbital interaction energy observed in the methyl complex. This strong orbital interaction, mostly based on forming a stronger M−L $\pi$-bond, is able to override the unfavorable non-orbital interaction component described above to give an overall preference for the Y-shaped coordination geometry.

**Model Studies and Predictions.** To further test our model and establish a relative scale for the energy components presented above, we conducted a series of computational experiments.

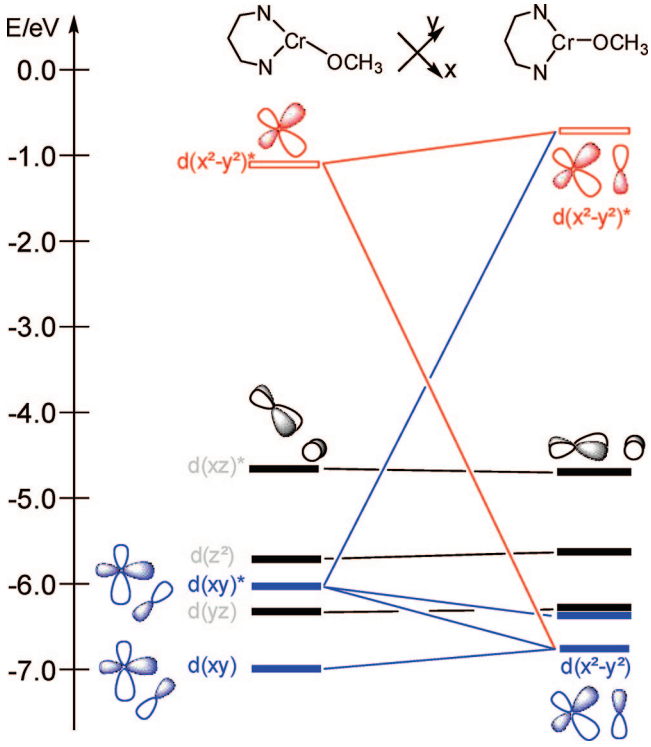


***Figure 8.*** Walsh diagram of the (nacnac′)Cr($OCH_3$) complex.

First, the putative Sc(II) $d^1$ complex (nacnac′)Sc(L) was analyzed as a model system. Whereas no such complex has been isolated, three coordinate Sc(II) complexes have often been invoked as reactive intermediates en route to formation of the short list of Sc(I) compounds.[37] Our expectation for the Sc(I) compounds is that the energetic discrimination of Y-shaped geometry based on non-orbital interaction terms should vanish, as the d-orbitals that introduce the asymmetric electronic structure described above are not occupied. In addition, the dramatic difference in orbital interaction energy between the T- and Y-geometry for the methoxy ligand should also vanish, as both the d($xy$) and d($x^2-y^2$) orbitals can now act as $\pi$-acceptors, making both ligand positions equivalent in orbital interaction terms. The energy components summarized in Table 5 indicate that the Y-shaped coordination geometry is energetically preferred regardless of the third ligand. For (nacnac′)-Sc($CH_3$), the Y-shaped geometry is favored by 7.3 kcal/mol overall, and we found a preference of 4.1 kcal/mol for (nacnac′)Sc($OCH_3$). As anticipated from the conceptual understanding discussed above, our calculations show that the non-orbital interaction penalty for Y-shaped chromium complex disappeared and the Y-shaped scandium complex is preferred by −5.0 and −5.9 kcal/mol for the methyl and methoxy complexes, respectively. The orbital interaction components of the Sc complex also show the anticipated behavior and display only a very small difference between the two coordination geometries for both the methyl and methoxy complexes. The orbital interaction energy of the methyl ligand in Y-coordination geometry is lower by −2.3 kcal/mol compared to the T analogue, which is essentially identical to −2.6 kcal/mol energy difference observed for the Cr analogue. The methoxy ligand interacts slightly stronger with the metal fragment in the T-shaped arrangement by 1.7 kcal/mol. It was noted in the latter chromium complex that the orbital energy was the dominating term with an energy difference of 12.0 kcal/mol.

Another putative model that further highlights the features controlling the energetics and structure of the (nacnac)M framework is (nacnac′)Mn($CH_3/OCH_3$), providing a Mn(II) $d^5$ analogue. Again, a restricted number of low-coordinate Mn(II) complexes in a nacnac-type ligand framework has been studied in the past, but a monomeric, three-coordinate Mn(II) complex has not been reported to date.[38−40] As all d-orbital-dominated

(37) Sc(I) complexes are exceedingly rare. (a) Beetstra, D. J.; Meetsma, A.; Hessen, B.; Teuben, J. H. *Organometallics* **2003**, *22*, 4372–4374. (b) Neculai, A. M.; Neculai, D.; Roesky, H. W.; Magull, J.; Baldus, M.; ronesi, O.; Jansen, M. *Organometallics* **2002**, *21*, 2590–2592. (c) Neculai, A.-M.; Cummins, C. C.; Neculai, D.; Roesky, H. W.; Bunkoczi, G.; Walfort, B.; Stalke, D. *Inorg. Chem.* **2003**, *42*, 8803–8810. (d) Arnold, P. L.; Cloke, F. G. N.; Hitchcock, P. B.; Nixon, J. F. *J. Am. Chem. Soc.* **1996**, *118*, 7630–7631.

(38) Three-coordinate ate complexes of Mn(II) have been reported. (a) Putzer, M. A.; Neumüller, B.; Dehnicke, K.; Magull, J. *Chem. Ber.* **1996**, *129*, 715–719. (b) Seidel, W.; Burger, I. *Z. Chem.* **1977**, *17*, 31. (c) Barlett, R. A.; Olmstead, M. M.; Power, P. P.; Shoner, S. C. *Organometallics* **1988**, *7*, 1801–1806.

***Table 6.*** Computed Component for the Interaction between (nacnac′)Mn and $CH_3/OCH_3$ in T-Shape and Y-Shape (nacnac′)Mn($CH_3/OCH_3$)

| | (nacnac′)Mn($CH_3$) | | | (nacnac′)Mn($OCH_3$) | | |
|---|---|---|---|---|---|---|
| (in kcal/mol) | T-shaped | Y-shaped | Δ | T-shaped | Y-shaped | Δ |
| Pauli repulsion (PR) | 168.26 | 158.80 | −9.46 | 130.95 | 121.27 | −9.68 |
| electrostatic interaction (EI) | −281.72 | −278.63 | 3.09 | −201.40 | −197.39 | 4.01 |
| non-orbital interaction (PR+EI) | −113.45 | −119.83 | −6.38 | −70.45 | −76.12 | −5.67 |
| orbital interaction | −197.38 | −193.34 | 4.04 | −230.14 | −225.34 | 4.80 |
| total energy | −310.83 | −313.18 | −2.35 | −300.59 | −301.46 | −0.87 |

frontier MOs are half-filled in this case, we expect the same rationale outlined above to be valid in this class of example, leading to the same predictions, namely, that the Y-shaped coordination should be slightly favored from non-orbital contributions to the total energy and that the orbital interaction energies should be essentially the same for the Y- and T-coordination geometries. The energy components are enumerated in Table 6 and confirm our expectations. As seen for the Sc analogue, the Y-shaped geometry is favored based on non-orbital interaction energies by 6.4 and 5.7 kcal/mol in the methyl and methoxy complexes, respectively. The difference in orbital interaction energies between the Y- and T-coordination geometries is relatively small, but this results in the T-shaped geometry being favored by 4−5 kcal/mol for both ligands. The Mn complexes are predicted to favor the Y-shaped geometry for both ligands, with the two coordination geometries of the methoxy system being essentially isoenergetic ($<1$ kcal mol$^{-1}$).

## Conclusions

A combined experimental and computational study of a series of novel three-coordinate, neutral chromous complexes of the type (nacnac)Cr(X) has allowed for deriving a deep and precise understanding of how the coordination geometry is controlled by the electronic structure of the third ligand. We found that a Y-shaped geometry is encouraged with purely $\sigma$-donor ligands ($X^- =$ alkyls ranging from sterically imposing to the less hindered $CH_3$ group), while $\pi$-donors favor the Y-shaped geometry ($X^- =$ bulky $\pi$-donors such an as aryl oxide to the less hindered dimethylamide ligand). Applying a combination of theoretical analysis of these structures and molecular orbital analysis as a function of geometrical changes, we established that the variations between T- versus Y-shape geometries are mostly governed by electronic factors with steric effects playing only a secondary role. The Pauli repulsion discourages the Y-geometry for $\sigma$-donors, and good $\pi$-donor ligands endorse the Y-shaped structure, in general, because the unoccupied Cr(II) d($x^2-y^2$) orbital promotes a strong $\pi$-bonding interaction between the metal and $\pi$-donor ligands, whereas the singly occupied d($xy$) orbital discourages approaches from Lewis bases in the Y-shaped geometry. The conceptual understanding that we derived for the Cr(II) systems allowed us to predict the structure of unprecedented and hypothetical three-coordinate complexes of Sc(II) and Mn(II). Naturally, other hypothetical 3d metal systems having the (nacnac)M(II) surrogate could be predicted given our systematic approach to rationalizing the electronic factors behind three-coordinate environments. Being able to predict or discriminate between these two types of geometries will undoubtedly set a new precedence for the rational design of unsaturated metal frameworks having unique electronic and reactivity features. Efforts in our laboratory are currently attempting the synthesis of neutral, three-coordinate (nacnac)Mn(X) complexes to validate one of our theoretical predictions.

**Acknowledgment.** We thank the Dreyfus Foundation, the Alfred P. Sloan Foundation (D.J.M. and M.-H.B.), the Camille and Henry Dreyfus Foundation (Teacher-Scholar Award to D.J.M.), the Research Corporation (Cottrell Scholar Award to M.-H.B.), and the NSF (CHE-0348941, PECASE to D.J.M.; CHE-0645381 to M.-H.B.) for financial support. F.J.Z.-C. would like to thank to CONACYT and UAEH for supporting a short stay at Indiana University under the Grant J110.390/2006.

**Supporting Information Available:** Complete crystallographic data (complexes **1**−**7**), computed structures and energies, and experimental details (all relevant data for **1**−**7** and model compounds). This material is available free of charge via the Internet at http://pubs.acs.org.

JA803798B

(39) A three-coordinate Mn(I) complex has been reported. Chai, J.; Zhu, H.; Stuckl, A. C.; Roesky, H. W.; Magull, J.; Bencini, A.; Caneschi, A.; Gatteschi, D. *J. Am. Chem. Soc.* **2005**, *127*, 9201–9206.

(40) For examples of three-coordinate Mn(III) complexes, see: (a) Ellison, J. J.; Power, P. P.; Steven, C.; Shoner, S. C. *J. Am. Chem. Soc.* **1989**, *111*, 8044–8046. (b) Kralik, M. S.; Stahl, L.; Arif, A. M.; Strouse, C. E.; Ernst, R. D. *Organometallics* **1992**, *11*, 3617–3621.